CONF-900704--1

UCRL- 102497
PREPRINT

SHOCK TUBE IGNITION OF ISOMERS OF OCTANE

Alexander Burcat
William J. Pitz
Charles K. Westbrook

This paper was prepared for submission to
23rd Symposium (International) on Combustion
22-27 July, 1990, Orleans France

December 13, 1989

Lawrence Livermore National Laboratory

SHOCK TUBE IGNITION OF ISOMERS OF OCTANE

Alexander Burcat
Faculty of Aerospace Engineering
Technion - Israel Institute of Technology
Haifa, Israel

and

William J. Pitz and Charles K. Westbrook
Lawrence Livermore National Laboratory
Livermore, California 94550

UCRL--102497-1

DE90 005991

Abstract

Ignition delay time measurements were carried out behind reflected shock waves for three isomers of octane, including n-octane, 2,2,4-trimethyl pentane, and 2,3,4-trimethyl pentane, and for 1-octene. Initial concentrations of fuel, oxygen, and argon, and the post-shock temperature were varied systematically to establish the influences of these parameters on ignition delay time. A detailed chemical kinetic reaction mechanism was developed to interpret the experimental results. Overall agreement between experimental and computed results was very good, and the model was used to describe the elementary reaction paths by which these fuels ignite and kinetic differences between these closely related hydrocarbon fuels.

INTRODUCTION

Both the size and structure of a given hydrocarbon fuel molecule are very important in determining its overall rate of ignition. The influence of fuel size was examined for the C_1-C_5 n-alkanes [1-3], and extensions to n-octane test the predictive capabilities of kinetic models. In addition, some processes, such as intramolecular H atom abstraction reactions, become important only as the fuel molecule becomes as large as C_5-C_8. Fuel structure also plays an immense role in determining certain combustion properties for hydrocarbon fuels. For example, the straight-chain n-octane has an octane number of approximately zero, indicating a very strong tendency towards knocking behavior in internal combustion engines, while its isomeric form iso-octane is extremely knock resistant and has an octane rating of 100. The present work addresses the importance of fuel structure for large hydrocarbon fuels by comparing the ignition of isomers of octane under shock tube conditions, using a combined experimental and kinetic modeling approach.

There have been relatively few experimental studies of shock tube ignition of large hydrocarbon fuels, dealing primarily with n-heptane [4-7] and iso-octane [4]. Coats and Williams [7] carried out a simplified model analysis of their own experiments with n-heptane. More recent modeling studies [3,8-10] also examined ignition of selected C_7 and C_8 hydrocarbons in shock tubes.

EXPERIMENTAL

Ignition delay time measurements were performed with 2,2,4 tri-methyl-pentane, 2,3,4 tri-methyl-pentane, n-octane and 1-octene, in a single pulse stainless steel shock tube. Ignition delay time was defined as the time interval between the pressure rise from the reflected shock and the onset of pressure rise due to ignition. The shock tube is 54 mm in diameter and 4 m long, and the driven section is 2.5 m long. Mylar diaphragms of different gauges were used, which were burst by the helium driver gas pressure.

The sampling section, 0.25 m long, contained three Kistler 603A piezoelectric transducers. Two of them, located 0.2 m apart, measured the shock velocity, while the third gauge, located on the end plate, recorded the pressure history. All three signals were recorded using a Nicolet dual trace digital oscilloscope, with points recorded at 1 μsec intervals with 12-bit resolution. One trace was connected to the end plate transducer, while the other was connected to the other two transducers in parallel.

The fuels used were Flucka pure reagents. Other gases were I.B. Miller oxygen and nitrogen (99% pure), Herzlyia argon (99% pure), and Airco pure grade helium, used without further purification. All gas mixtures were made manometrically in stainless steel containers, pressurized to ≈50 psia. To ensure thorough mixing of the gases, the mixtures were left for 48 hours before use, in the containers. Since some of the reagents, like n-octane, have low vapor pressures, there was a concern that part of the vapors might condense on the walls of the container. Therefore the steel containers were replaced with 20-liter glass bulbs, with the overall mixture pressure kept sub-atmospheric. Reflected shock temperatures were calculated using standard techniques and recently compiled thermochemical data [11].

EXPERIMENTAL RESULTS

A total of 489 experiments were performed, consisting of 172 experiments with 1-octene (1-C_8H_{16}), 129 experiments with 2,2,4 tri-methyl pentane (iso-octane), 30 experiments with 2,3,4 tri-methyl pentane (3-C_8H_{18}), and 158 experiments with n-octane. The different mixtures used for experimentation are listed in Table I, chosen so that the parameters in the empirical ignition delay equation

$$\tau = \beta\ [\mathrm{Fuel}]^a [\mathrm{O_2}]^b [\mathrm{Ar}]^c\ \mathrm{sec}$$

could be unambiguously determined. Statistical least-squares analyses of these data developed overall correlations, in kcal-mol-cm^3-s units, of

$$\tau = 10^{-11.52}\exp(20.6/RT)[n\text{-}C_8H_{18}]^{-0.11\pm.14}[O_2]^{-0.30\pm.11}[Ar]^{-.40\pm.40}\text{sec.}$$

$$\tau = 10^{-12.65}\exp(25.3/RT)[i\text{-}C_8H_{18}]^{0.36\pm.10}[O_2]^{-1.34\pm.15}[Ar]^{-.04\pm.46}\text{sec.}$$

$$\tau = 10^{-12.74}\exp(37.9/RT)[1\text{-}C_8H_{16}]^{0.93\pm.07}[O_2]^{-1.27\pm.10}[Ar]^{-.45\pm.16}\text{sec.}$$

These correlations are compared with experimental results in Figs. 1-3. Correlations for 1-octene and iso-octane are very good, while that for n-octane is fair. Because of the limited number of experiments carried out for 2,3,4 trimethyl pentane, no overall correlation was determined.

NUMERICAL MODEL AND KINETIC REACTION MECHANISM

The numerical model used is the HCT code [12], which solves the coupled conservation equations of mass, momentum, and energy. For the present conditions, constant volume, adiabatic conditions are assumed. The same model and boundary conditions have been used in the past [2,3,9,10,13-15] to analyze shock tube experiments.

The chemical kinetic reaction mechanism was based on previous studies of the oxidation of large hydrocarbon fuel molecules, particularly n-heptane, n-octane, and iso-octane [9,16,17]. Due to limitations of space, the entire reaction mechanism of 119 species and 653 reactions is not included here, but it is given in detail in Reference 18.

The mechanism includes initiation, site-specific abstraction of H atoms from each type of fuel molecule, isomerization and thermal decomposition of the resulting alkyl radicals, and oxidation of the smaller hydrocarbon fragments, particularly olefins, to final products. These steps had already been identified and included in earlier models for n-octane and iso-octane [9,10,16], but no previous mechanism existed for 2,3,4 trimethyl-pentane. The present reaction mechanism for 1-octene is a subset of that for n-octane.

Most of the differences in ignition delay times among the three isomers of octane can be related to relative rates of production of H atoms during the decomposition of the fuel and the various octyl radicals. Generally, reaction paths that produce H atoms accelerate the overall rate of ignition of hydrocarbons at high temperatures, due to their impact on the

$$H + O_2 = O + OH$$

chain branching reaction, while paths that lead to relatively stable species such as methyl or allyl radicals tend to retard the rate of ignition.

The major initiation reactions for these fuels involve breaking a C - C bond. The resulting radical species then decompose rapidly via β-scission. The net results of this process for each fuel are:

$$n\text{-}C_8H_{18} \rightarrow 1\text{-}C_4H_9 + 1\text{-}C_4H_9 \rightarrow 4\ C_2H_4 + H + H \qquad \text{(a)}$$

$$\rightarrow 1\text{-}C_5H_{11} + nC_3H_7 \rightarrow 3\ C_2H_4 + CH_3 + CH_3 \qquad \text{(b)}$$

$$i\text{-}C_8H_{18} \rightarrow i\text{-}C_4H_9 + t\text{-}C_4H_9 \rightarrow iC_4H_8 + C_3H_6 + CH_3 + H \qquad \text{(a)}$$

$$\rightarrow neo\text{-}C_5H_{11} + iC_3H_7 \rightarrow iC_4H_8 + C_3H_6 + CH_3 + H \qquad \text{(b)}$$

$$3\text{-}C_8H_{18} \rightarrow x\text{-}C_5H_{11} + iC_3H_7 \rightarrow 2C_4H_8 + C_3H_6 + CH_3 + H$$

$$1\text{-}C_8H_{16} \rightarrow 1\text{-}C_4H_9 + C_4H_7 \rightarrow 2\ C_2H_4 + C_4H_7 + H \qquad \text{(a)}$$

$$\rightarrow 1\text{-}C_5H_{11} + C_3H_5 \rightarrow 2\ C_2H_4 + C_3H_5 + CH_3 \qquad \text{(b)}$$

Some of these fuels have two important routes for thermal decomposition. For $n\text{-}C_8H_{18}$ and $1\text{-}C_8H_{16}$, the reactions labeled (a) produce H atoms and accelerate ignition in the computations, while the (b) reactions produced CH_3 and retarded ignition. These trends were used to refine the model rate expressions. For the large hydrocarbon fuels examined here, thermal decomposition reactions account for a considerable fraction of the total rate of fuel consumption, even after the radical pool is established. This is in distinct contrast to the case of smaller fuels such as methane, ethane [2], and propane [14], where most of the fuel consumption is accomplished through radical attack.

Following an initiation period, a radical pool is established which consumes fuel and other hydrocarbon species through H atom abstraction reactions. For all of the fuels considered here, site-specific H atom abstraction reaction rates have not been studied experimentally, so the rates must be estimated. This procedure [19] consists simply of assuming that the rate of abstraction depends only on the nature of the abstracting radical, the type of C-H bond being broken (i.e. primary, secondary, or tertiary), and the number of logically identical H atoms in the molecule. In Table II the reaction rate expressions used for each type of C-H bond are summarized.

It is essential to distinguish between H atom abstraction from logically distinct sites in each fuel molecule. For example, the 2-octyl radical from n-octane decomposes via sequential β-scission steps to

$$2\text{-}C_8H_{17} \rightarrow C_3H_6 + 1\text{-}C_5H_{11} \rightarrow C_3H_6 + C_2H_4 + C_2H_4 + CH_3$$

while the 3-octyl radical produces

$$3\text{-}C_8H_{17} \rightarrow 1C_4H_8 + 1\text{-}C_4H_9 \rightarrow 1C_4H_8 + C_2H_4 + C_2H_4 + H \quad .$$

Both octyl radicals are produced by breaking a secondary C-H bond, so the rates of those H atom abstraction processes are assumed equal, but subsequent decomposition of the octyl radicals yields different products, including the H atom in the case of $3\text{-}C_8H_{17}$ and CH_3 in the case of $2\text{-}C_8H_{17}$, which have opposite influences on the overall rate of ignition.

In the present model, octyl radicals can isomerize through internal H atom abstraction steps. Rates of isomerization depend on the strain energy of the ring-like transition state, the nature of the C-H bond being broken, and the number of equivalent H atoms at each available site [19].

Oxidation of smaller hydrocarbon fragments is computed using reaction mechanisms developed previously for the combustion of smaller fuels. The H_2-O_2-CO submechanism, and the submechanisms for oxidation of the C_1 - C_2 species are based strongly on a review by Warnatz [20]. The C_3 - C_6 sections are based on recent modeling studies [21].

One reaction not included in the Warnatz review but which is often included in reaction mechanisms for C_1 - C_2 hydrocarbons is

$$CH_3 + HO_2 = CH_3O + OH$$

which leads to considerable chain branching and accelerates the overall rate of ignition of the present octanes, due to the subsequent decomposition of CH_3O into $CH_2O + H$. In the present model, it was very difficult to reproduce the experimental induction time observations without inclusion of this reaction; induction times computed without this reaction were generally too long by factors ranging from 4 to 10.

COMPUTATIONAL RESULTS

Comparisons between computed and experimental values for the ignition delay time are summarized in Figs. 4-5. For each fuel (except for 2,3,4 trimethyl pentane), one lean, one rich, and one near-stoichiometric mixture is included. The individual reactions which had the greatest influence on the computed results were determined by sensitivity analysis, the results of which are illustrated in Table III. The sensitivity coefficient shown is the logarithm of the ratio of the ignition delay time computed with the rate of the reaction doubled in both forward and reverse directions, to that computed with the baseline mechanism. A negative value indicates that the increased rate expression results in a shorter ignition delay time, while a positive value indicates that the larger rate expression produces a longer ignition delay time.

Most significantly, the most sensitive reactions are those associated with the H_2-O_2-CO and the C_1-C_2 reaction submechanisms, consistent with observations [22] for oxidation of large hydrocarbons in flames. However, there is no sensitivity to variations in the rate of

$$CO + OH = CO_2 + H$$

which plays a prominent role in determining laminar burning velocities in flames. Reactions involving the fuel and other large hydrocarbon species have relatively small sensitivities. The computed results are especially sensitive to the rate of the $H+O_2 = O+OH$ chain branching reaction, and most of the other sensitivies can be interpreted easily in terms of their impact on the H atom pool and the $H+O_2$ branching reaction. For example, the second and third reactions in Table III lead to H atom production from thermal decomposition of the CH_3O and C_2H_3 radicals, respectively. Therefore, increasing the rates of these reactions leads to a shorter computed value for the ignition delay time. The importance of the $OH+HO_2$ reaction and its positive sensitivity coefficient is due to its chain termination role and its consumption of two radicals which otherwise react with C_2H_4 and CH_3 to produce H atoms. While formally a chain propagating step, reaction of H atoms with octane molecules has a positive sensitivity coefficient indicating that when these rates are increased the overall rate of ignition decreases. This occurs because these reactions compete for H atoms with the chain branching $H+O_2$ reaction.

DISCUSSION

N-octane is a linear chain with only primary and secondary C-H bonds, 2-3-4-trimethyl-pentane is highly branched and contains only primary and tertiary C-H bonds, and iso-octane is also highly branched and includes a mixture of primary, secondary, and tertiary C-H bonds. These fuels therefore provide a rather wide range of kinetic features.

Analysis of the product distributions of fuel decomposition and the thermal decomposition of the various alkyl radicals produced by H atom abstraction permits us to rank the present fuels in terms of their relative production of H atoms and CH_3 radicals. The greatest production of H atoms is expected in n-octane, followed by 2,3,4 trimethyl pentane, and followed in turn by iso-octane. When comparable mixtures of these fuels with oxygen and argon are examined, either experimentally or with the numerical model, the same ordering is observed; n-octane ignites fastest, followed by 2,3,4 trimethyl pentane and then by iso-octane. The fuel 1-octene is found to ignite slightly faster than any of the branched octanes but slower than n-octane.

The numerical model was used to predict the overall activation energy for the ignition of each fuel. With the relative fuel, oxygen, and argon concentrations held fixed, the initial temperature was varied over a range from about 1200 to 1600 K, and the ignition delay time was computed using the detailed kinetic reaction mechanism. The overall activation energies for the different fuels in the present study were found to be 39.0 kcal/mole in the case of iso-octane, 40.3 kcal/mole for 2,3,4 trimethyl pentane, 40.6 kcal/mole for n-octane, and 39.5 kcal/mole for 1-octene. Recall that the statistical analysis of the experimental results described earlier yielded overall activation energies ranging from 20 kcal/mol to 37.9 kcal/mol. The computational result suggests that the temperature dependence for ignition of large hydrocarbon fuels is relatively insensitive to variations in fuel molecule structure; an approximate value of 40 kcal/mole could be estimated for any large hydrocarbon, branched or straight-chain. This temperature dependence is the result primarily of the reaction submechanisms for the smaller hydrocarbon species, especially those in the H_2-O_2 and the C_1 and C_2 submechanisms.

This combined experimental and computational study of octane isomers and 1-octene shows that molecular structure plays an important role in determining overall rates of combustion at shock tube temperatures and pressures. The techniques used here for estimation of site-specific H atom abstraction rates have been shown to provide needed kinetic data in cases where experimental data do not yet exist.

Sensitivity analysis demonstrated that the greatest attention should be given to reaction rates and product distributions of reactions involving relatively small hydrocarbon species. This is true for the H_2-O_2 submechanism, for small olefins such as ethene, propene, and isobutene, and for the relatively stable small radical species like methyl and allyl. Reactions of these species provide most of the control over radical pool levels, which in turn determine the chain branching properties of the reaction mechanism. However, the present results also show that, in contrast with reaction mechanisms of small hydrocarbon fuels, thermal decomposition reactions of large fuel molecules provide a large fraction of the rate of fuel consumption, and accurate values for these decomposition rates would be helpful in refining this kinetic model.

The present study shows that it is well within current capabilities to model ignition of a significant range of large, structurally complex fuels. It is important to note that the reaction mechanisms developed in this work are appropriate for high temperature conditions only, including shock tube and flame propagation environments. Extensions to lower temperatures to deal with applications such as engine knock would require the addition of many other families of chemical species and elementary reaction paths. Steps necessary to make these model extensions have been developed [16], but that topic is beyond the scope of the present paper.

ACKNOWLEDGMENTS

The experimental part of this work was supported by a grant from the United States - Israel Binational Science Foundation. The computational part of this work was supported by the U. S. Department of Energy, Office of Energy Utilization Research, Division of Energy Conversion and Utilization Technologies, and by the U. S. Department of Energy, Office of Energy Research, Office of Basic Energy Sciences, Division of Chemical Sciences. This work was carried out in part under the auspices of the U. S. Department of Energy by the Lawrence Livermore National Laboratory under contract NO. W-7405-ENG-48.

References

1. Burcat, A., Scheller, K., and Lifshitz, A., Combust. and Flame 16, 29 (1971).
2. Westbrook, C. K., Combust. Sci. and Technol. 20, 5 (1979).
3. Westbrook, C. K., and Pitz, W. J., Shock Waves and Shock Tubes, D. Bershader and R. Hanson, eds., p. 287, Stanford University Press, Stanford, California, 1986.
4. Vermeer, D. J., Meyer, J. W., and Oppenheim, A. K., Combust. and Flame 18, 327 (1972).
5. Ciezki, H., and Adomeit, G., Sixteenth International Symposium on Shock Tubes and Shock Waves, 1987.
6. Burcat, A., Farmer, R. F., and Matula, R. A., Thirteenth International Symposium on Shock Tubes and Waves, Niagara Falls, 1981.
7. Coats, C. M., and Williams, A., Seventeenth Symposium (International) on Combustion, p. 611, The Combustion Institute, Pittsburgh, 1979.
8. Esser, C., Maas, U., and Warnatz, J., International Symposium on Diagnostics and Modeling of Combustion in Reciprocating Engines, 1985.
9. Westbrook, C. K., and Pitz, W. J., in Complex Chemical Reaction Systems, J. Warnatz and W. Jager, eds., Springer-Verlag, Berlin-Heidelberg, 1987
10. Westbrook, C. K., and Pitz, W. J., Ind. and Eng. Chem. Prod. Res. and Dev. 25, 159 (1986).

11. Burcat, A., Chapter 8 in Chemistry of Combustion, W. C. Gardiner, Jr., ed., Springer-Verlag, (1984).
12. Lund, C. M., Lawrence Livermore Laboratory report UCRL-52504, 1978.
13. Westbrook, C. K., and Dryer, F. L., Combust. Sci. and Technol. 20, 125 (1979).
14. Westbrook, C. K., and Pitz, W. J., Combust. Sci. and Technol. 37, 117 (1984).
15. Westbrook, C. K., Dryer, F. L., and Schug, K. P., Nineteenth Symposium (International) on Combustion, p. 153, The Combustion Institute, Pittsburgh, 1983.
16. Westbrook, C. K., Warnatz, J., and Pitz, W. J., Twenty-Second Symposium (International) on Combustion, p. 893, The Combustion Institute, Pittsburgh, 1989.
17. Axelsson, E. I., Brezinsky, K., Dryer, F. L., Pitz, W. J., and Westbrook, C. K., Twenty-First Symposium (International) on Combustion, p. 783, The Combustion Institute, Pittsburgh, 1988.
18. Burcat, A., Pitz, W. J., and Westbrook, C. K., Fall Meeting of the Western States Section of The Combustion Institute. Lawrence Livermore National Laboratory report UCRL-102001, October 1989.
19. Westbrook, C. K., and Pitz, W. J., SAE Trans. Section 7 96, 559 (1988).
20. Warnatz, J., Chapter 5 in Chemistry of Combustion, W. C. Gardiner, Jr., ed., Springer-Verlag, New York (1984).
21. Thornton, M. M., Malte, P. C., Pitz, W. J., and Westbrook, C. K., Combust. and Flame 72, 45 (1988).
22. Warnatz, J., Combust. Sci. and Technol. 34, 177 (1983).

TABLE I. Experimental conditions of fuel-oxygen-argon mixtures.

Group	Fuel	Fuel%	O_2%	Ar%	P torr	No. of shocks
A1	C_8H_{16}	1.	12.	87.	85.	33.
A2	C_8H_{16}	2.	24.	74.	55.	18.
A3	C_8H_{16}	2.	24.	74.	75.	20.
A4	C_8H_{16}	0.75	24.	75.25	60.	10.
A5	C_8H_{16}	0.75	23.27	76.	80.	39.
A6	C_8H_{16}	2.	9.	89.	80.	23.
A7	C_8H_{16}	0.5	6.	93.5	170.	29.
B1	n-C_8H_{18}	1.	12.4	86.6	80.	10.
B2	n-C_8H_{18}	1.	13.2	85.8	80.	8.
B3	n-C_8H_{18}	0.4	12.65	86.95	85.	11.
B4	n-C_8H_{18}	1.	3.	96.	80.	21.
B5	n-C_8H_{18}	2.	24.	74.	70.	24.
B6	n-C_8H_{18}	1.	6.	93.	80.	28.
B7	n-C_8H_{18}	0.33	12.5	87.17	80.	20.
B8	n-C_8H_{18}	0.4	12.65	86.95	160.	14.
B9	n-C_8H_{18}	0.7	8.93	90.37	75.	8.
B10	n-C_8H_{18}	1.	12.5	86.5	60.	14.
C1	2,2,4C_8H_{18}	1.	12.5	86.5	75.	52.
C2	2,2,4C_8H_{18}	1.	13.2	85.8	70.	8.
C3	2,2,4C_8H_{18}	0.33	12.5	87.17	75.	11.
C4	2,2,4C_8H_{18}	1.	6.	93.	75.	11.
C5	2,2,4C_8H_{18}	1.	5.	94.	70.	19.
C6	2,2,4C_8H_{18}	2.	25.	73.	50.	28.
D1	2,3,4C_8H_{18}	1.	12.5	86.5	75.	18.
D2	2,3,4C_8H_{18}	2.	25.	73.	79.	12.

Table II

Site-specific rates of H atom abstraction per C-H bond
Abstracting radical species are indicated at the left,
the site is shown at the top
Units are cm^{3}-mol^{-1}-s^{-1}, activation energies are in cal/mol

	primary	secondary	tertiary
H	$9.4\times10^{6}T^{2}\exp(-7700/RT)$	$4.55\times10^{6}T^{2}\exp(-5000/RT)$	$1.26\times10^{14}\exp(-7300/RT)$
O	$7.3\times10^{5}T^{2.4}\exp(-5500/RT)$	$2.35\times10^{5}T^{2.5}\exp(-2230/RT)$	$1.1\times10^{13}\exp(-3280/RT)$
OH	$1.75\times10^{9}T^{0.97}\exp(-1590/RT)$	$2.34\times10^{7}T^{1.61}\exp(-40/RT)$	$5.73\times10^{10}T^{0.51}\exp(-63/RT)$
CH_3	$2.15\times10^{11}\exp(-11600/RT)$	$2.0\times10^{11}\exp(-9500/RT)$	$1.0\times10^{11}\exp(-7900/RT)$
HO_2	$1.9\times10^{12}\exp(-19400/RT)$	$1.7\times10^{12}\exp(-17000/RT)$	$3.0\times10^{12}\exp(-14400/RT)$

Table III

Sensitivity coefficients for reactions in ignition of isomers of octane. Species labeled C_8H_{18} refer to the isomer at the top of each respective column. For each reaction indicated, both forward and reverse reaction rates were doubled, leaving the equilibrium constant unchanged. For H atom abstraction reactions from octane, rates for all possible H atom sites were simultaneously multiplied by factors of 2.

Reaction			Sensitivity Coefficient		
			nC_8H_{18}	iC_8H_{18}	$3C_8H_{18}$
$H + O_2$	=	$O + OH$	-0.23	-0.34	-0.33
$CH_3 + HO_2$	=	$CH_3O + OH$	-0.08	-0.04	-0.07
$C_2H_4 + OH$	=	$C_2H_3 + H_2O$	-0.08	-0.01	-0.02
$OH + HO_2$	=	$H_2O + O_2$	0.07	0.03	0.04
$C_8H_{18} + H$	=	$C_8H_{17} + H_2$	0.05	0.07	0.06
C_8H_{18}	=	alkyl products	-0.05	-0.01	-0.01
$CH_3 + H$	=	CH_4	0.04	0.07	0.08
$CH_3 + O_2$	=	$CH_2O + OH$	-0.03	-0.14	-0.10
$CH_3 + CH_3$	=	C_2H_6	0.02	0.04	0.03
$HCO + M$	=	$H + CO + M$	-0.01	0.03	0.01
$HCO + O_2$	=	$CO + HO_2$	0.01	-0.04	-0.03
$C_8H_{18} + OH$	=	$C_8H_{17} + H_2O$	0.01	0.02	0.02
$H + O_2 + M$	=	$HO_2 + M$	-0.00	-0.03	-0.01

FIGURE CAPTIONS

1. Overall ignition dependence of 1-octene (1-C_8H_{16}) from statistical correlation of experimental results.

2. Overall ignition dependence of 2,2,4 trimethyl pentane (iso-octane) from statistical correlation of experimental results.

3. Overall ignition dependence of n-octane (n-C_8H_{18}) from statistical correlation of experimental results.

4. Comparison between experimentally measured (symbols) and computed (lines) ignition delay times for iso-octane (top) and n-octane (bottom). Dotted lines and squares refer to lean mixtures, solid lines and circles refer to near-stoichiometric mixtures, and dashed lines and triangles refer to rich mixtures.

5. Comparison between experimentally measured (symbols) and computed (lines) ignition delay times for 2,3,4 trimethyl pentane (top) and 1-octene (bottom). The mixture for 2,3,4 trimethyl pentane is stoichiometric, and for 1-octene, the dotted line and squares refer to the lean mixture, the solid line and circles refer to the stoichiometric mixture, and the dashed line and triangles refer to the rich mixture.

Figure 1

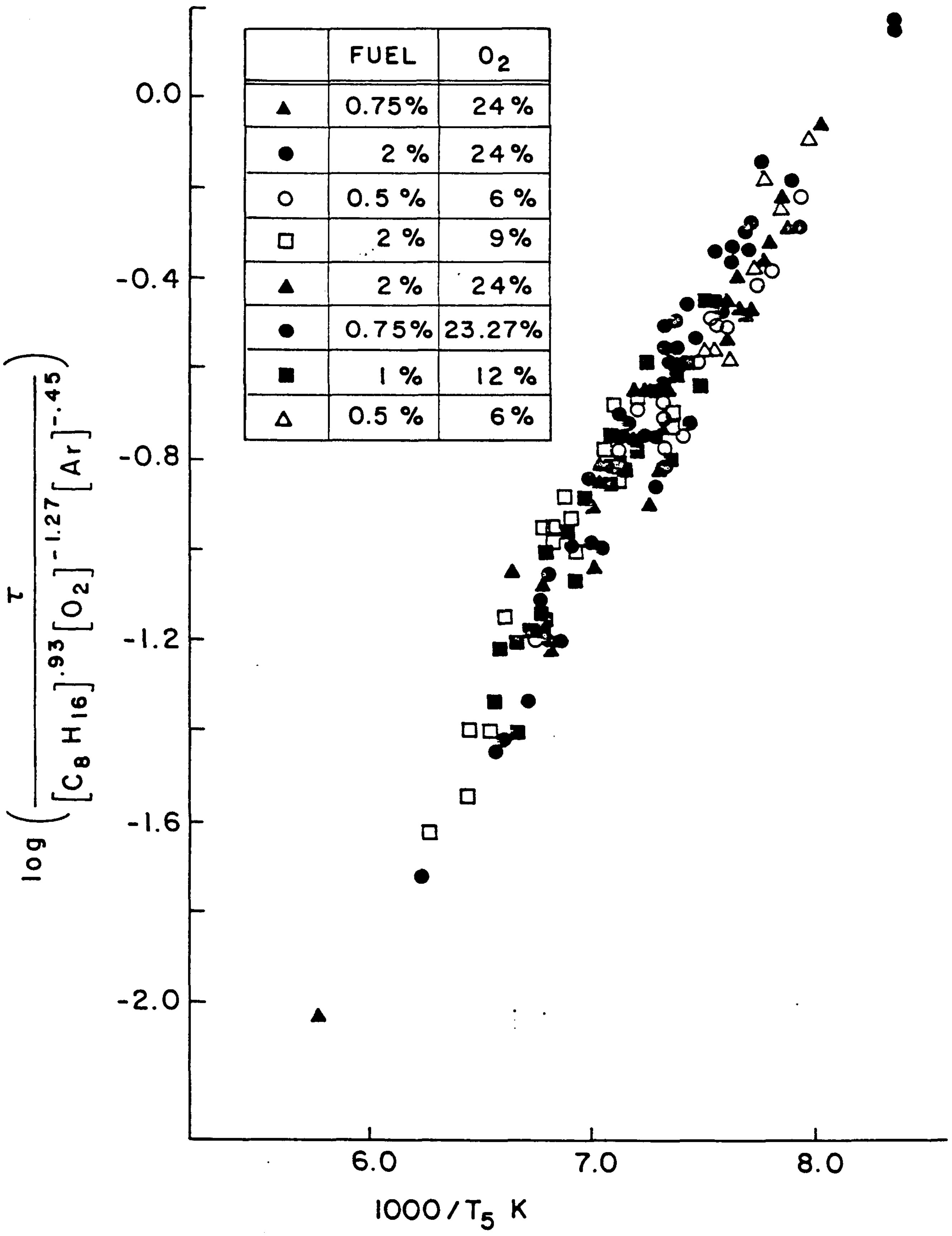
FUEL
O_2
▲ 0.75% 24%
● 2% 24%
○ 0.5% 6%
□ 2% 9%
▲ 2% 24%
● 0.75% 23.27%
■ 1% 12%
△ 0.5% 6%
0.0
-0.4
-0.8
-1.2
-1.6
-2.0
$\log\left(\frac{\tau}{[C_8H_{16}]^{.93}[O_2]^{-1.27}[Ar]^{-.45}}\right)$
6.0
7.0
8.0
$1000/T_5$ K

Figure 2

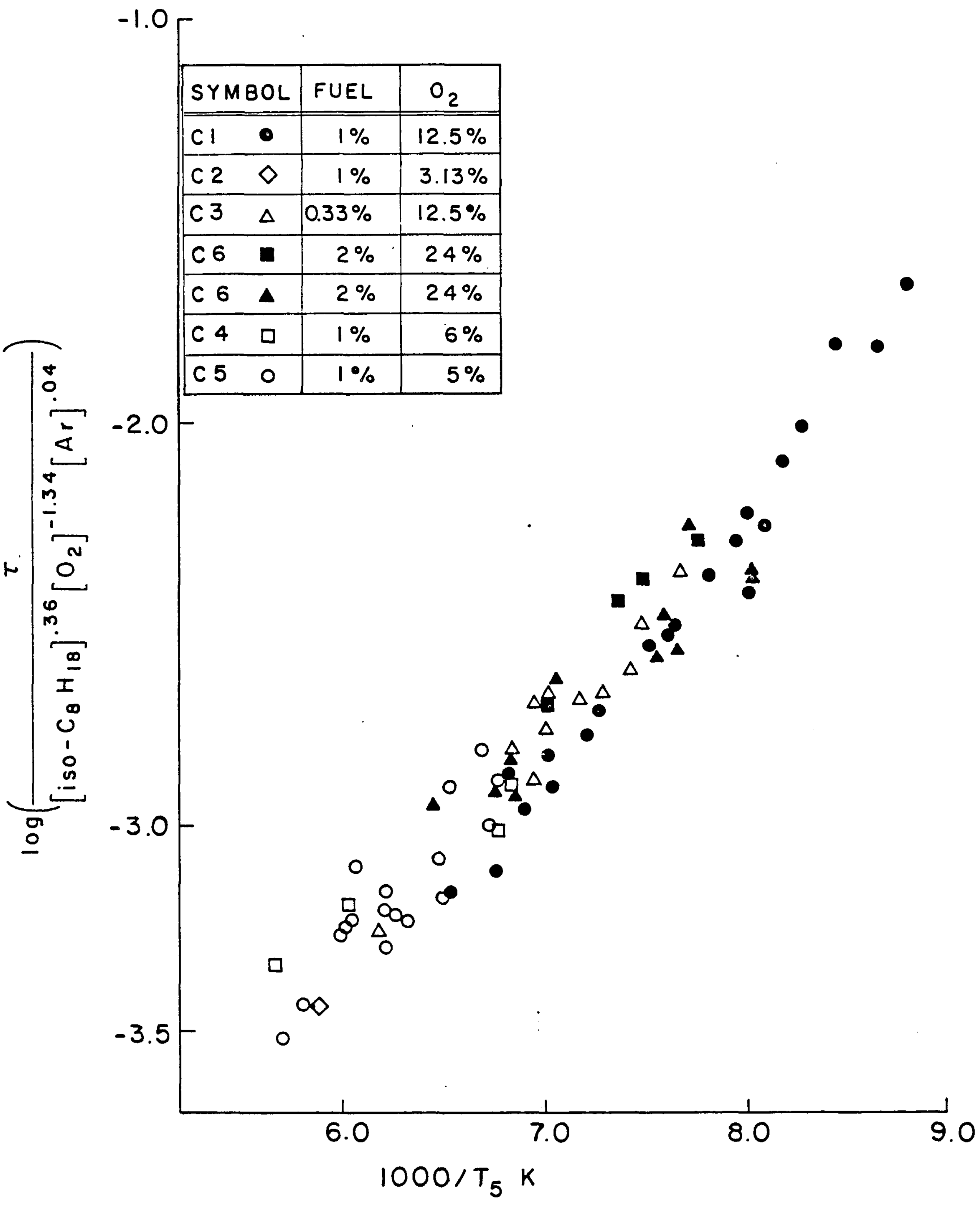
SYMBOL | FUEL | O_2
C1 ● 1% 12.5%
C2 ◇ 1% 3.13%
C3 △ 0.33% 12.5%
C6 ■ 2% 24%
C6 ▲ 2% 24%
C4 □ 1% 6%
C5 ○ 1% 5%
-1.0
-2.0
-3.0
-3.5
6.0
7.0
8.0
9.0
$\log\left(\frac{\tau}{[\text{iso-}C_8H_{18}]^{.36}[O_2]^{-1.34}[Ar]^{.04}}\right)$
$1000/T_5$ K

Figure 3

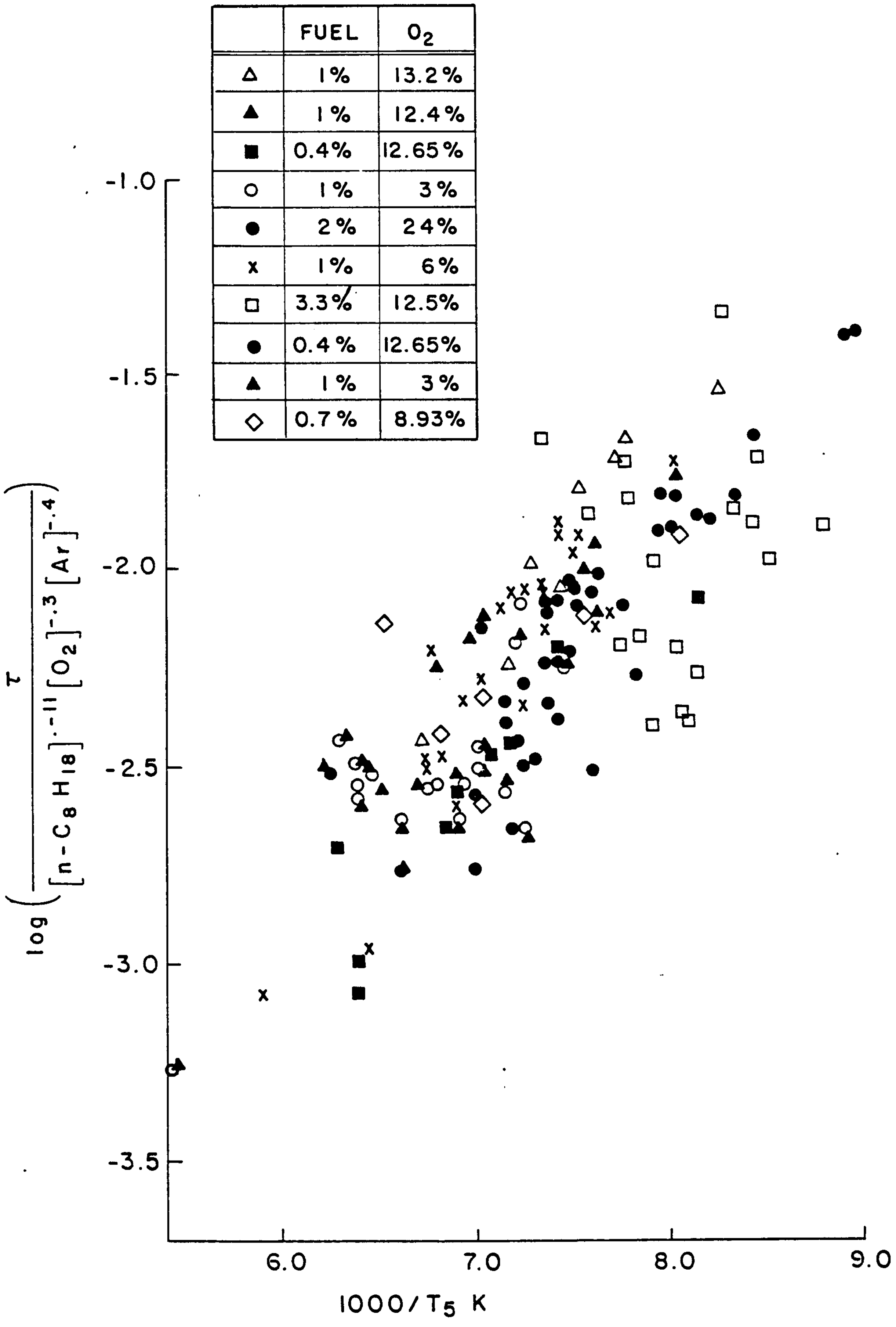
FUEL
O_2
△ 1% 13.2%
▲ 1% 12.4%
■ 0.4% 12.65%
○ 1% 3%
● 2% 24%
x 1% 6%
□ 3.3% 12.5%
● 0.4% 12.65%
▲ 1% 3%
◇ 0.7% 8.93%
-1.0
-1.5
-2.0
-2.5
-3.0
-3.5
6.0
7.0
8.0
9.0
1000/T_5 K
$\log\left(\frac{\tau}{[n\text{-}C_8H_{18}]^{-.11}[O_2]^{-.3}[Ar]^{-.4}}\right)$

Figure 4

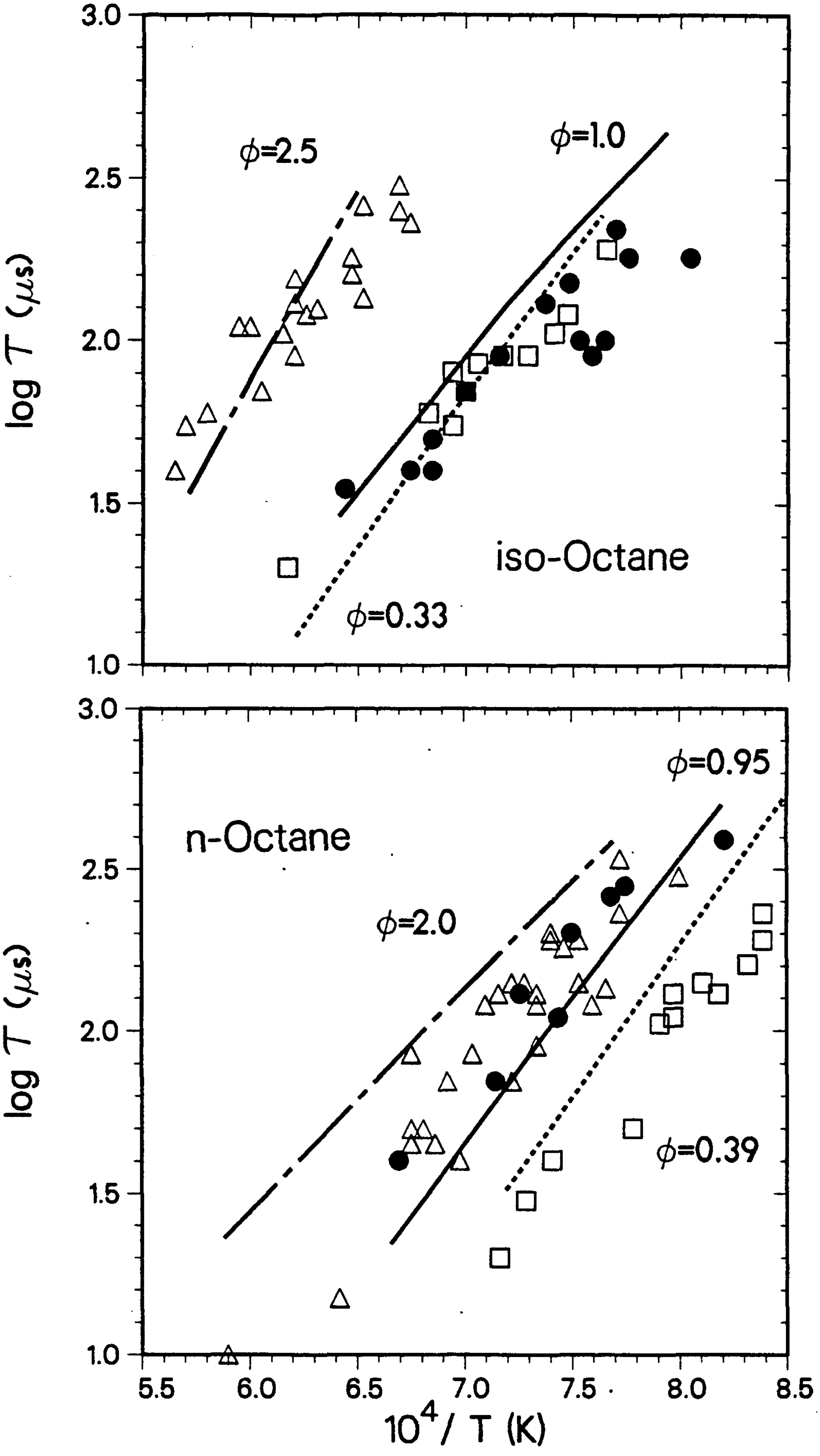

3.0
2.5
2.0
1.5
1.0
log τ (μs)
φ=2.5
φ=1.0
φ=0.33
iso-Octane
3.0
2.5
2.0
1.5
1.0
log τ (μs)
n-Octane
φ=0.95
φ=2.0
φ=0.39
5.5
6.0
6.5
7.0
7.5
8.0
8.5
10⁴/ T (K)

Figure 5

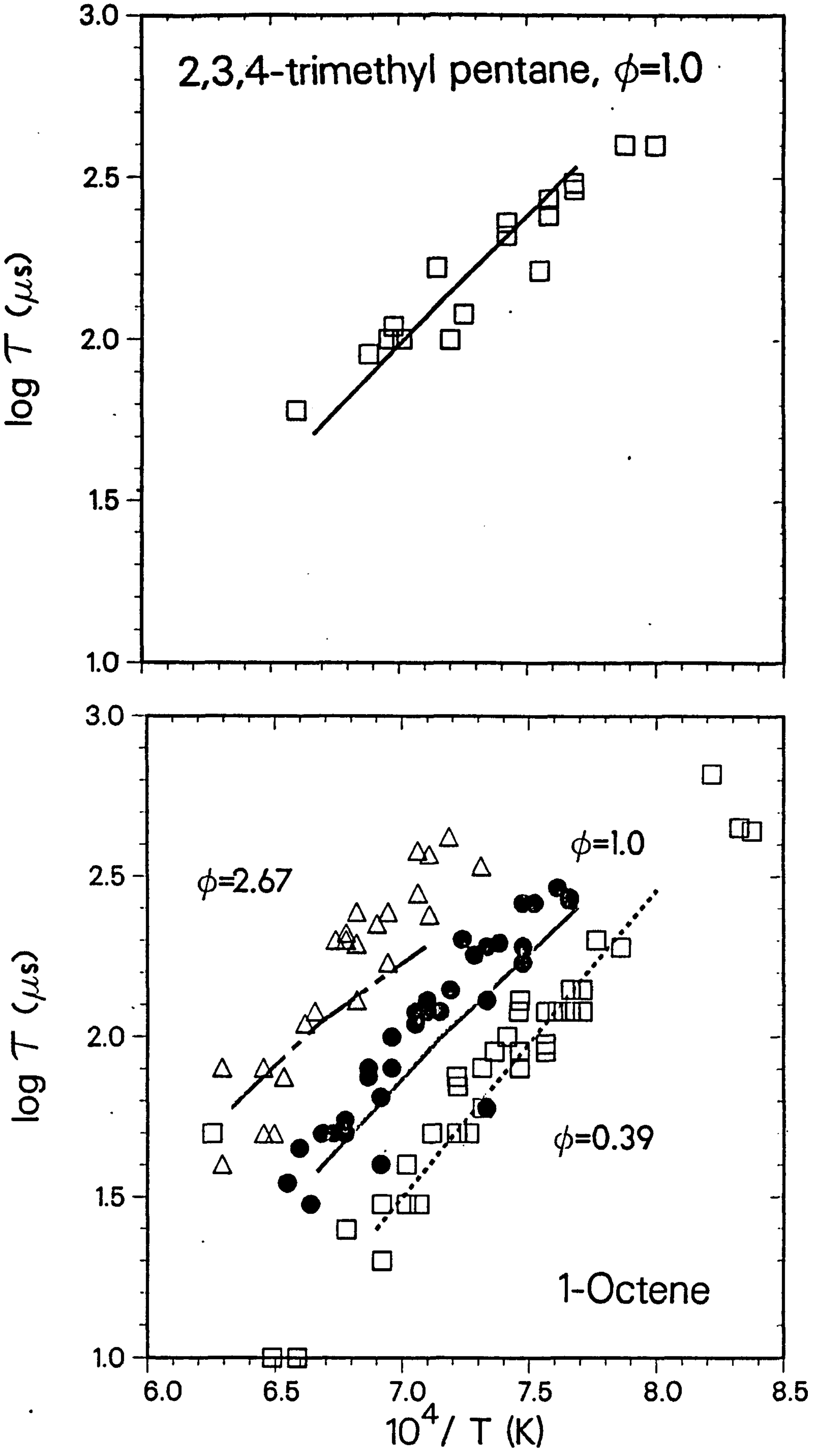

2,3,4-trimethyl pentane, ϕ=1.0
log τ (μs)
3.0
2.5
2.0
1.5
1.0
ϕ=2.67
ϕ=1.0
ϕ=0.39
1-Octene
6.0
6.5
7.0
7.5
8.0
8.5
10^4/ T (K)

Technical Information Department · Lawrence Livermore National Laboratory
University of California · Livermore, California 94551